Optical impulse response of silica microspheres: Complementary approach to whispering-gallery-mode analysis

Hugo Bergeron, Jean-Raphaël Carrier, Vincent Michaud-Belleau, Julien Roy, Jérôme Genest, and Claudine Nì. Allen*
Centre d'Optique, Photonique et Laser (COPL), Université Laval, Québec, Canada, G1V 0A6
(Received 18 March 2013; published 20 June 2013)

We use frequency comb interferometry to simultaneously obtain the optical impulse responses and wide-band transmission spectra of silica microspheres, as they together provide a more complete description of light dynamics inside the resonator. The grouping of periodic cavity ring-down pulses in the impulse response provides confirmation that small asphericities give rise to a precession of the orbit of the light pulse propagating along the inner surface of the microcavity. This effect also strongly depends on coupling conditions. Moreover, we notice the presence of secondary pulses associated with modes of higher radial quantum number. All these features bring valuable information on the optical properties of microspheres.

DOI: 10.1103/PhysRevA.87.063835 PACS number(s): 42.79.Gn, 42.79.Pw, 42.79.Sz

I. INTRODUCTION

Optical microresonators are key elements in several areas of fundamental and applied sciences, such as optoelectronics, cavity quantum electrodynamics, optical filtering and switching, wavelength-division multiplexing, biosensing, and nonlinear optics [1]. When using dielectric microspheres as sensors, the mechanism for detection is often the spectral shift of whispering-gallery-mode (WGM) resonant frequencies. This technique is capable of detecting various changes in the sphere's environment such as analyte adsorption [2–4], refractive index [5] and temperature [6] variations, and accelerations [7]. Still, specific information on the nature of the perturbation is generally limited since most analyses consider only a narrow frequency band. On the other hand, simultaneously monitoring several WGMs on a wide spectral band increases the number of parameters available, enabling a better characterization of the environment probed by the sphere [8–10].

To overcome the challenge of analyzing a large number of modes, time-domain analysis can be considered. To do so, many methods have been developed in the last decades. For instance, cavity ring-down of a light pulse is a well-known phenomenon [11] used to measure resonator characteristics, especially when its energy storage is very efficient [12]. Other methods also exist based on the sweeping of the resonator length [13,14] or of the input laser frequency [15–17]. Using pulses to probe a resonator is a more direct way to measure its impulse response, but basic modulators produce pulses lasting longer than the round-trip time: a careful analysis accounting for the coupling properties is thus required [18,19]. Durations shorter than the round-trip time can be achieved with femtosecond laser sources [20,21], adding the benefit of a larger bandwidth exciting multiple modes at once. Moreover, using radio frequency modulation, the optical impulse response in the time domain can be readily obtained from the phase-sensitive transmission or reflection spectroscopy of resonators [22,23]. It should be noted that whenever the Hilbert transform is applicable, the frequency spectrum modulus alone suffices to compute the impulse response [24]. Recently, the powerful technique of frequency comb interferometry [25] has been applied to directly probe the impulse response of glass microspheres [26]. In spite of all this progress, an elegant description of the observed light pulse dynamics in both time and frequency domains is still missing.

In this paper, we fully relate the features of the transmission spectrum (frequency-domain analysis) to the optical impulse response (time-domain analysis) of single silica microspheres. We first describe the propagation of light via the impulse response, which can be intuitively linked to the pulse trajectory in the microresonator. Precession, along with cavity ring-down, are observed with improved accuracy and thoroughly explained. We then make the comparison with the frequency domain. Since the time-domain data are obtained with an unprecedented level of detail, we resolve slightly different group delays introduced by different radial modes. We finally discuss how modifications of the coupling conditions affect the various features observed in the impulse response and the frequency spectrum.

II. METHODS AND MATERIAL

The complete setup and its dispersion correction algorithm is essentially the same as in [26]. The diameters of the silica microspheres vary from 60 to 300 μm. Using a micrometric translation stage, a single microsphere is brought into contact with a 4-μm tapered fiber to induce coupling between microsphere and fiber modes. They stay in contact due to various adhesion forces [27].

The microspheres are probed with an interferometric setup using two frequency comb lasers (Fig. 1). One comb excites the microresonator producing a periodized version of its impulse response. The second comb is used to optically sample the probe signal, such as to take a sample at a different and known time delay for each repetition. The optical impulse response, which is convolved with the mutual coherence function of the two combs, is obtained over a duration of more than 10 ns, with a resolution of about 80 fs.

This 10-ns window comes from the 100-MHz repetition rate of the combs defining the spectral mode spacing and hence the spectral resolution of the measurement. The main strength of the setup is its high measurement rate, allowing to obtain up to

*claudine.allen@phy.ulaval.ca

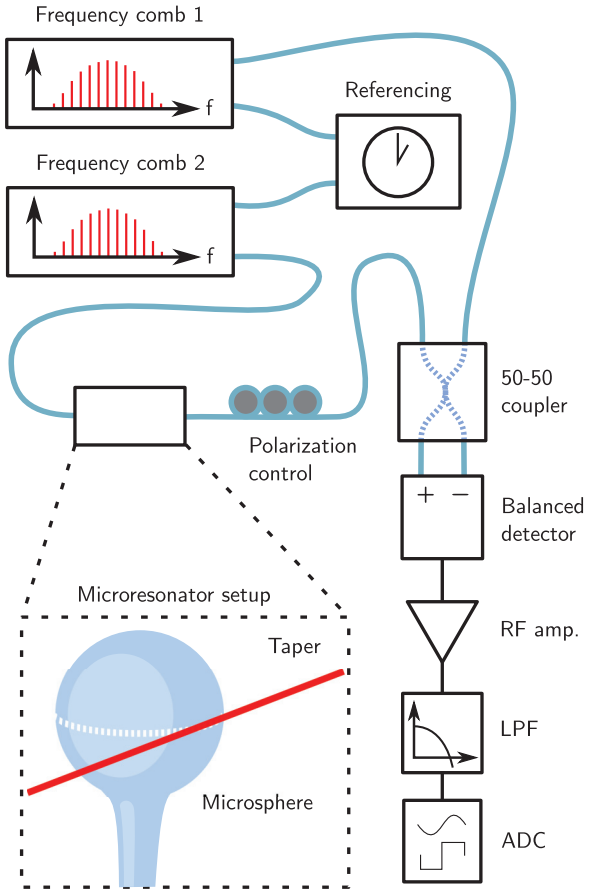

FIG. 1. (Color online) This interferometric measurement technique provides the optical impulse response of the probed microsphere, from which the complex spectrum can be deduced over the bandwidth of the combs, which are centered around 194 THz. The setup includes two frequency comb lasers. One laser is sent through the tapered fiber where it is coupled to the microsphere. The other laser, having a slightly different repetition rate, is sent through a reference fiber. The two signals are then combined in a fiber coupler. Both combs are also sent to a referencing stage to determine accurately the timings of the measurements [25]. LPF: low pass filter; ADC: analog to digital converter; RF amp.: radio frequency amplifier.

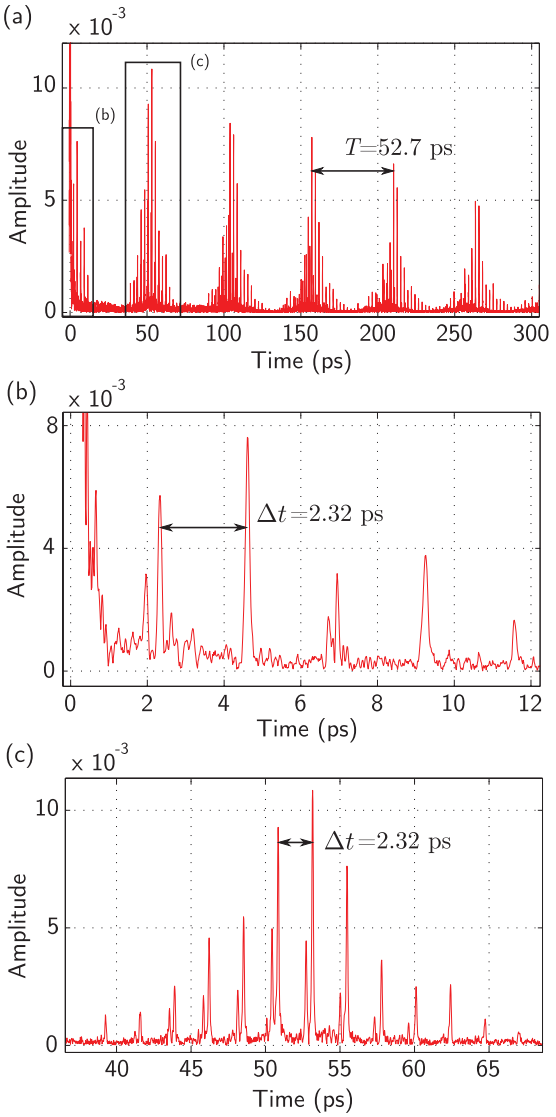

FIG. 2. (Color online) Optical impulse response of a 155-μm silica microsphere as measured with our dual frequency comb setup. The amplitude of the impulse response is normalized with respect to the pulse that stays in the fiber and reaches the detector without having entered the sphere. $\Delta t = 2.32$ ps is the time the light pulse takes to complete a single revolution. $T = 52.7$ ps is the observed period between recurring groups of pulses. Zooms on the (b) first pulses and on the (c) first recurring cluster are shown.

100 spectra per second over the full 100-nm comb bandwidth. Several modes can thus be tracked simultaneously in spectral amplitude and phase, as well as in the time-domain impulse response. If needed, successive measurements can be averaged to improve the signal-to-noise ratio.

III. RESULTS

The impulse response is connected to the complex spectrum by the Fourier transform. In the spectral domain, the interferometric measurement yields the resonator transfer function (in magnitude and phase) multiplied by the combs' cross-spectral density. In the time domain, the measurement consists of the resonator's impulse response convolved with the combs' mutual coherence function. These two complementary views provide different perspectives on the resonator's physics. Whereas the spectrum directly shows the resonant modes, the time-domain analysis better highlights the temporal evolution of the electromagnetic field within the cavity. Figure 2 shows the measured impulse response of a 155-μm silica microsphere and Fig. 3, its associated transmission spectrum. Many features are visible in the impulse response.

First, the impulse response presents a gradual decrease in intensity as time advances [Fig. 2(a)]. This effect is the time-domain counterpart of the width of resonances in the frequency spectrum: it is thus quantified by the quality factor. A microsphere having modes with higher Q factors will exhibit a longer ring-down in its impulse response. Since the measured Q factor depends not only on cavity loss but also

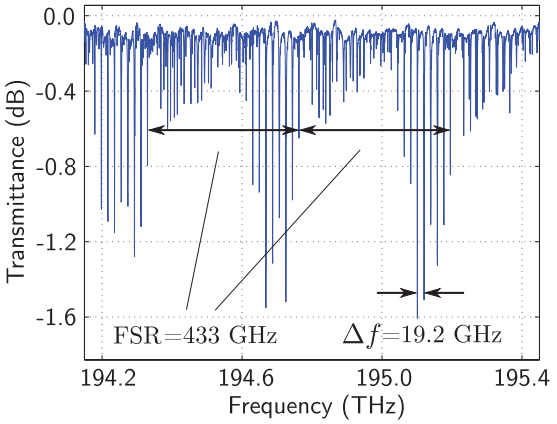

FIG. 3. (Color online) Transmission spectrum of a 155-μm silica microsphere, computed from its impulse response shown in Fig. 2. FSR = 433 GHz is the spacing between consecutive $\ell = |m|$ modes, whereas $\Delta f = 19.2$ GHz is the spacing between m modes.

on resonator-fiber coupling, increasing the fraction of energy coupled from the tapered fiber to the resonator shortens the cavity ring-down. The signal-to-noise ratio of the impulse response must therefore be sacrificed to observe a longer ring-down, as less light is initially coupled into the resonator.

The first peak in Fig. 2(b) (out of scale) corresponds to light that stays in the fiber and that directly reaches the detector without coupling in the resonator. The observed recurring peaks come from the coupled pulse traveling along the circumference of the sphere [20,28], recoupling with the tapered fiber after each of the first few revolutions. In this geometrical paradigm, the detected pulses are thus separated by Δt, which is the time taken by pulses to circumnavigate the sphere. This group delay is linked to the resonator modal structure through the group velocity v_g

$$\Delta t = \frac{2\pi a}{v_g} = \frac{2\pi a}{d\omega/dk}, \tag{1}$$

where a is the radius of the sphere, ω is the angular frequency, and k is the wave number. To estimate $d\omega/dk$, one needs to project the pulse onto the sphere's orthogonal modes. When only considering degenerate m modes of a perfect sphere with radial quantum number[1] $n = 1$, the group velocity becomes

$$v_g = \frac{d\omega}{dk} \approx \frac{\Delta\omega_\ell}{\Delta k} = \frac{2\pi(f_{\ell+1} - f_\ell)}{[(\ell+1) - \ell]/a}. \tag{2}$$

Equation (1) then becomes

$$\Delta t \approx \frac{1}{f_{\ell+1} - f_\ell} = \frac{1}{\mathrm{FSR}}. \tag{3}$$

The quantity $f_{\ell+1} - f_\ell$ is often named the free spectral range (FSR) in analogy to the constant mode spacing of Fabry-Perot resonators. Obviously, the resonators used in our experiment cannot be made perfectly spherical. Consequently, m modes appear within each FSR of the computed spectrum, as shown in Fig. 3. Nevertheless, the equation $\Delta t \times \mathrm{FSR} = 1$ holds. For instance, with our 155-μm sphere, $\Delta t = 2.32$ ps and FSR = 433 GHz as seen in Figs. 2 and 3. When dispersion is low, the FSR can be regarded as constant for a given n. Our data suggest that dispersion is negligible in our experiment: the pulses do not undergo significant widening in the impulse responses.

Another interesting feature found in the measured impulse responses is the existence of groups of pulses. Figure 2(c) displays one of these clusters. This phenomenon is caused by a precessional effect: the slight ellipticity of the resonator affects the propagation of the energy within the cavity. After each revolution around the cavity, the light pulse does not come back exactly where it was one revolution before. In other words, the trajectory of the light pulse precesses: it takes several revolutions before the coupling with the fiber becomes optimal again. The precession creates pulse clusters with a period T, as shown in Fig. 2. This period is directly related by the Fourier transform to the average separation Δf between two consecutive m modes: $T\Delta f = 1$. This is confirmed by the 155-μm sphere used in our experiment having $T = 52.7$ ps and $\Delta f = 19.2$ GHz. The separation Δf is, in general, a function of geometry and quantum numbers n, ℓ, and m. For instance, the frequencies of nondegenerate m modes in a spheroidal resonator are given by [29]

$$f_{\ell m} \approx f_\ell \left[1 - \frac{e}{6}\left(1 - \frac{3m^2}{\ell(\ell+1)}\right)\right], \tag{4}$$

where e is a constant that quantifies the ellipticity in the polar direction and f_ℓ is the frequency of the degenerate ℓth mode as if the resonator had been a perfect sphere. The quantity Δf is obtained by differentiating with respect to m

$$\Delta f \approx \Delta m \frac{df_{\ell m}}{dm} = e\left(\frac{f_\ell}{\ell}\right)\left(\frac{m}{\ell+1}\right), \tag{5}$$

where $\Delta m = 1$. Our data show that Δf is nearly constant over the measured spectrum bandwidth. Looking at Eq. (5) leads to the same conclusion: since the microsphere is coupled near its equator, the average ratio $m/(\ell+1) \approx m/\ell$ is close to unity. Furthermore, the fact that the FSR is nearly constant in the measured spectrum implies a constant f_ℓ/ℓ ratio. Precession in the context of WGMs has already been studied [28,30–32]. However, previous work focused mostly on precession involving a single or a limited number of modes. In our setup, all modes within the combs' bandwidth are excited at the same time. The many evenly spaced m modes give rise to a time-dependent precession with period $T = 1/\Delta f$. To illustrate this, Fig. 4 compares the trajectories of a Gaussian pulse built from modal superposition in perfect and deformed spheres. An asymptotic expansion was used to obtain the solutions of the WGM characteristic equation [33], Eq. (4) providing the perturbed mode frequencies in the deformed case. It should be noted that the explanation for the precession given here is not the same as the one provided in [28], where the pulse's unclosed trajectory lies on a constant plane. Our results show that the orbital plane precesses with a period T. Our explanation implies that no such precession must occur when all m modes are degenerated. The same principle applies to system having no quantum number m, such as ring resonators [24].

[1]The quantum numbers are such that m is the number of oscillations along the equator, $\ell - |m|$ is the number of nodes on a meridian, and n is the number of maxima in the radial direction.

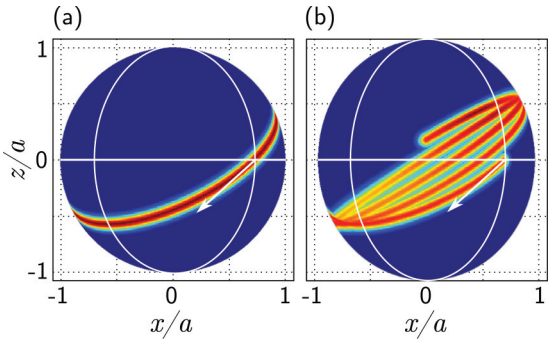

FIG. 4. (Color online) Computer simulation showing the path taken by a Gaussian pulse in (a) spherical and (b) spheroidal resonators of mean radii a, for four revolutions. Decomposing the pulse into its modal components, multiplying them by $\exp(j\omega_{\ell m}t)$, then summing them back yields the trajectory of the pulse. The frequency spacing between m modes in a deformed sphere causes a precession in the pulse's orbit.

The high temporal resolution of our experimental setup makes secondary pulses visible in the optical impulse response, as shown in Fig. 5. After several revolutions in the microsphere, the light pulse has split, giving rise to additional pulses of lower intensity. More of these additional pulses can be distinguished for larger microspheres, as shown in Fig. 5(b). We demonstrate here that the additional pulses are formed by modes having $n > 1$. For each possible value of n, a set of modes can be formed from all modes having this particular radial quantum number value. Each set of modes has its own FSR, and thus its own group delay. To illustrate this, the frequencies of transverse electric (TE) and transverse magnetic (TM) modes with $n \in [1,6]$ were computed using

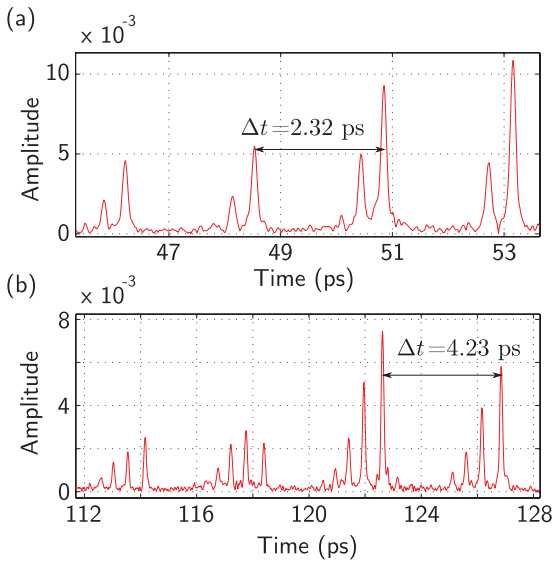

FIG. 5. (Color online) Secondary pulses can be seen in the optical impulse response of silica microspheres, and are more numerous for larger resonators. (a) The pulses after 20, 21, 22, and 23 revolutions around a 155-μm microsphere are shown. (b) The pulses after 27, 28, 29, and 30 revolutions around a 280-μm microsphere are shown. The apparent splitting is caused by the dependence of the FSR on the radial quantum number n.

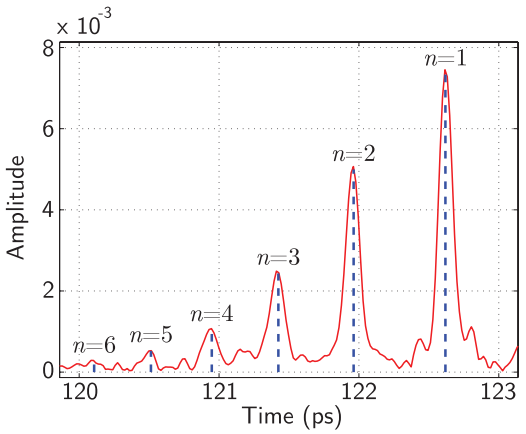

FIG. 6. (Color online) The computed arrival times of secondary pulses, each formed by a set of modes having the same radial quantum number n (blue dashed lines) fit the experimental data (red curve). The figure shows a split pulse after its 29th revolution around a 280-μm microsphere.

the WGM characteristic equation. The analysis was limited to modes being in the spectral range of our setup. FSRs were then estimated for each value of n and each polarization state. Finally, the expected arrival times of pulses were computed with Eq. (3). Figure 6 shows the agreement between this computation and experimental data after 29 revolutions in a 280-μm sphere. On one hand, the difference between TE and TM pulse arrival times is not observed as it is of the order of few femtoseconds, thus smaller than the resolution of our setup. On the other hand, a change in the radial mode number has a more significant and clearly visible effect. For the selected diameter and revolution number, the experiment yields a 0.65-ps delay between $n = 1$ and $n = 2$ pulses while the computation predicts a 0.66-ps delay.

Up to this point, we only considered the case where a microsphere was coupled to a tapered fiber in a specific configuration: the fiber touches the sphere at and parallel to its equator. Changing these conditions affects the features discussed previously, each to a different degree.

The position of the tapered fiber relative to the microsphere can be described by two parameters: the latitude on the sphere at which there is contact with the fiber and the angle the fiber forms with the equator of the sphere. Figure 7 shows that the latitude barely affects the time Δt taken by the light pulse to circumnavigate the cavity. Instead, in aspherical resonators, the latitude significantly changes the period of precession T by modifying the shape of the unclosed path taken by the light pulse. The groups of pulses are closer to each other when the tapered fiber is further from the equator. Also, the number of pulses within each group is significantly reduced at higher latitudes. The coupling conditions determine the quantity of energy transferred from the tapered fiber to the different cavity modes [34–38]. Increasing the latitude at which the sphere is in contact with the tapered fiber allows WGMs of higher $\ell - |m|$ values to be coupled. Because lifting the m-mode degeneracy depends on quantum numbers n, ℓ, and m, high-latitude (high $\ell - |m|$) modes need not have the same spectral separation Δf as low-latitude (low $\ell - |m|$) modes. This explains why the rate of precession differs for both situations. The latitude

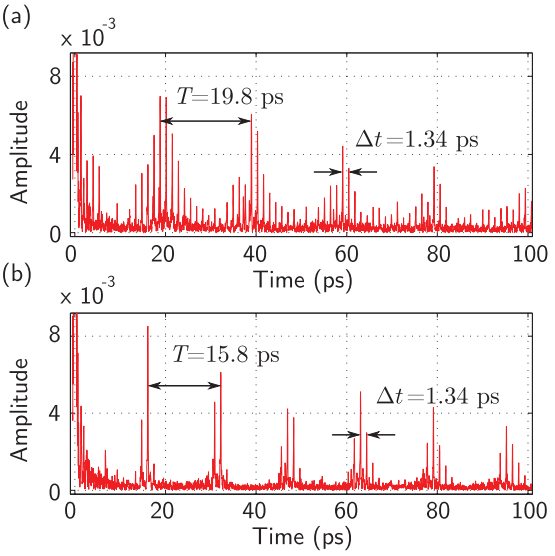

FIG. 7. (Color online) The period of precession T decreases when the contact between the optical tapered fiber and the microsphere is not at the equator of the latter, while the delay between each pulse Δt remains roughly the same. Also, there are fewer pulses in each cluster. (a) shows the impulse response of a 100-μm sphere coupled at its equator to the tapered fiber, whereas for (b) the latitude of the contact is of about 30°.

was modified both ways, north and south from the equator (Fig. 1), yielding similar results.

A modification of the coupling angle affects the impulse response in the same way as a change in latitude, but to a smaller extent. The angle must at least be 20° for these effects to be observed at all.

IV. CONCLUSION

The optical impulse response of a microsphere provides a complementary perspective to the typical WGM transmission spectrum that proves very useful to consolidate the comprehension of the dynamics of light in spheroidal cavities. The time-domain approach is better suited to describe the propagation of light pulses inside a resonator, along with its precession caused by asphericities. It clearly shows features that are difficult to see or quantify in the spectral domain, such as a significant presence of modes of higher radial quantum number. In addition to asphericities, the coupling conditions between the tapered fiber and the microsphere modify the precession trajectory and thus the impulse response and spectrum.

The study of the time-domain features described in this article sheds a new light on spherical resonators. It complements the information provided by the transmission spectrum, which is also available with our measurements. We believe that combining time- and frequency-domain measurements can only reinforce the knowledge basis on microresonators and their interaction with their surroundings.

ACKNOWLEDGMENTS

The authors thank Simon Potvin, Reno Lessard, Patrick Larochelle, Maxime Charlebois, Jean-Daniel Deschênes, Olivier Rousseau-Cyr, and Professor Réal Tremblay for their precious contributions. This paper could not have been made without their collaboration, nor without financial support from Le Fonds de recherche du Québec Nature et technologies (FRQNT).

[1] T. M. Benson, S. V. Boriskina, P. Sewell, A. Vukovic, S. C. Greedy, and A. I. Nosich, in *Frontiers in Planar Lightwave Circuit Technology*, NATO Science Series II: Mathematics, Physics and Chemistry, Vol. 216 (Springer, Netherlands, 2006), pp. 39–70.

[2] F. Vollmer, D. Braun, A. Libchaber, M. Khoshsima, I. Teraoka, and S. Arnold, Appl. Phys. Lett. **80**, 4057 (2002).

[3] S. Arnold, M. Khoshsima, I. Teraoka, S. Holler, and F. Vollmer, Opt. Lett. **28**, 272 (2003).

[4] F. Vollmer, S. Arnold, and D. Keng, Proc. Nat. Acad. Sci. USA **105**, 20701 (2008).

[5] N. M. Hanumegowda, C. J. Stica, B. C. Patel, I. White, and X. Fan, Appl. Phys. Lett. **87**, 201107 (2005).

[6] C.-H. Dong, L. He, Y.-F. Xiao, V. R. Gaddam, S. K. Ozdemir, Z.-F. Han, G.-C. Guo, and L. Yang, Appl. Phys. Lett. **94**, 231119 (2009).

[7] J.-P. Laine, C. Tapalian, B. E. Little, and H. A. Haus, Sensors and Actuators A: Physical **93**, 1 (2001).

[8] A. Francois and M. Himmelhaus, Appl. Phys. Lett. **92**, 141107 (2008).

[9] M. Charlebois, A. Paquet, L. S. Verret, K. Boissinot, M. Boissinot, M. G. Bergeron, and C. N. Allen, Sensors Journal, IEEE **13**, 229 (2013).

[10] T. Le, A. Savchenkov, N. Yu, L. Maleki, and W. H. Steier, Appl. Opt. **48**, 458 (2009).

[11] A. F. Harvey, *Microwave Engineering* (Academic, London, 1963).

[12] G. Rempe, R. J. Thompson, H. J. Kimble, and R. Lalezari, Opt. Lett. **17**, 363 (1992).

[13] K. An, C. Yang, R. R. Dasari, and M. S. Feld, Opt. Lett. **20**, 1068 (1995).

[14] J. Poirson, F. Bretenaker, M. Vallet, and A. Le Floch, J. Opt. Soc. Am. B **14**, 2811 (1997).

[15] I. S. Grudinin, V. S. Ilchenko, and L. Maleki, Phys. Rev. A **74**, 063806 (2006).

[16] A. A. Savchenkov, A. B. Matsko, V. S. Ilchenko, D. Strekalov, and L. Maleki, Phys. Rev. A **76**, 023816 (2007).

[17] S. Trebaol, Y. Dumeige, and P. Féron, Phys. Rev. A **81**, 043828 (2010).

[18] G. S. Pandian and F. E. Seraji, IEEE Proc. J **138**, 235 (1991).

[19] Y. Dumeige, S. Trebaol, L. Ghisa, T. K. N. Nguyên, H. Tavernier, and P. Féron, J. Opt. Soc. Am. B **25**, 2073 (2008).

[20] J.-P. Wolf, Y. L. Pan, G. M. Turner, M. C. Beard, C. A. Schmuttenmaer, S. Holler, and R. K. Chang, Phys. Rev. A **64**, 023808 (2001).

[21] T. Siebert, O. Sbanski, M. Schmitt, V. Engel, W. Kiefer, and J. Popp, Opt. Commun. **216**, 321 (2003).

[22] N. Uehara, A. Ueda, K. Ueda, H. Sekiguchi, T. Mitake, K. Nakamura, N. Kitajima, and I. Kataoka, Opt. Lett. **20**, 530 (1995).
[23] B. J. J. Slagmolen, M. B. Gray, K. G. Baigent, and D. E. McClelland, Appl. Opt. **39**, 3638 (2000).
[24] Y. Gottesman, D. G. Rabus, E. V. K. Rao, and B.-E. Benkelfat, IEEE Photonics Technol. Lett. **21**, 1399 (2009).
[25] J.-D. Deschênes, P. Giaccari, and J. Genest, Opt. Express **18**, 23358 (2010).
[26] V. Michaud-Belleau, J. Roy, S. Potvin, J.-R. Carrier, L.-S. Verret, M. Charlebois, J. Genest, and C. N. Allen, Opt. Express **20**, 3066 (2012).
[27] K.-T. Wan, D. T. Smith, and B. R. Lawn, J. Am. Ceram. Soc. **75**, 667 (1992).
[28] R. W. Shaw, W. B. Whitten, M. D. Barnes, and J. M. Ramsey, Opt. Lett. **23**, 1301 (1998).
[29] H. M. Lai, P. T. Leung, K. Young, P. W. Barber, and S. C. Hill, Phys. Rev. A **41**, 5187 (1990).
[30] J. M. Hartings, J. L. Cheung, and R. K. Chang, Appl. Opt. **37**, 3306 (1998).
[31] J. C. Swindal, D. H. Leach, R. K. Chang, and K. Young, Opt. Lett. **18**, 191 (1993).
[32] M. L. Gorodetsky and V. S. Ilchenko, Opt. Commun. **113**, 133 (1994).
[33] S. Schiller, Appl. Opt. **32**, 2181 (1993).
[34] C.-L. Zou, Y. Yang, C.-H. Dong, Y.-F. Xiao, X.-W. Wu, Z.-F. Han, and G.-C. Guo, J. Opt. Soc. Am. B **25**, 1895 (2008).
[35] B. E. Little, J.-P. Laine, and H. Haus, J. Lightwave Technol. **17**, 704 (1999).
[36] M. J. Humphrey, E. Dale, A. T. Rosenberger, and D. K. Bandy, Opt. Commun. **271**, 124 (2007).
[37] Y. Xu, Y. Li, R. K. Lee, and A. Yariv, Phys. Rev. E **62**, 7389 (2000).
[38] H. A. Haus, *Waves and Fields in Optoelectronics* (Prentice Hall, Saddle River, NJ, 1984).